



Deposited via The University of Leeds.

White Rose Research Online URL for this paper:

<https://eprints.whiterose.ac.uk/id/eprint/167752/>

Version: Accepted Version

Article:

Al-Gailani, A, Sanni, O, Charpentier, TVJ et al. (2021) Inorganic fouling of heat transfer surface from potable water during convective heat transfer. Applied Thermal Engineering, 184. 116271. p. 116271. ISSN: 1359-4311

<https://doi.org/10.1016/j.applthermaleng.2020.116271>

© 2020, Elsevier. This manuscript version is made available under the CC-BY-NC-ND 4.0 license <http://creativecommons.org/licenses/by-nc-nd/4.0/>.

Reuse

This article is distributed under the terms of the Creative Commons Attribution-NonCommercial-NoDerivs (CC BY-NC-ND) licence. This licence only allows you to download this work and share it with others as long as you credit the authors, but you can't change the article in any way or use it commercially. More information and the full terms of the licence here: <https://creativecommons.org/licenses/>

Takedown

If you consider content in White Rose Research Online to be in breach of UK law, please notify us by emailing eprints@whiterose.ac.uk including the URL of the record and the reason for the withdrawal request.

Inorganic Fouling of Heat Transfer Surface from Potable Water during Convective Heat Transfer

Amthal Al-Gailani^{a*}, Olujide Sanni^a, Thibaut V. J. Charpentier^b, Richard Crisp^c, Jantinus H. Bruins^d and Anne Neville^a

^a School of Mechanical Engineering, University of Leeds, Leeds, LS2 9JT, England

^b School of Chemical and Process Engineering (SCAPE), University of Leeds, Leeds, LS2 9JT, England

^c Fernox Limited, Woking, Surrey, GU21 5RW, England

^d WLN, Glimmen, 9756 AD, Netherlands

Abstract

In this work, inorganic fouling of the heat transfer surfaces from potable water has been studied using a once-through flow cell to visualize and follow the deposition processes. The effects of surface material and flow rate on the amount and morphology of deposits have been investigated. The scale which formed on surfaces mainly consists of two distinct regions; smooth and flat layer and a rough calcium carbonate layer. It also revealed that the scaling tendency on copper and aluminium is much greater than on stainless steel. Finally, the complex effect of flow rate on scale formation is also discussed.

Keywords: Heat transfer; Crystallization fouling; Potable water; Aluminium; Magnesium; Calcium carbonate.

Introduction

Inorganic fouling, the formation of unwanted deposits either on the heated surfaces in contact with the solution or in bulk fluid, occurs as a consequence of supersaturation of salt. The formation of

inorganic scale is thermodynamically possible when the aqueous solution is supersaturated with one of the sparingly soluble salts such as calcium carbonate CaCO_3 , sulphate salts of calcium, magnesium hydroxide $\text{Mg}(\text{OH})_2$, etc [1]. These deposits increase the resistance to heat transfer and reduce flow area of the working fluids in industrial, commercial and domestic systems [2-4]. The increasing resistance to heat flow and the high system pressure drop increase the energy consumption and maintenance cost and lower the durability of the system [5]. Fouling has long been a concern in domestic appliances such as electric boilers, gas boilers, steam irons, washing machines, dishwashers, coffee makers and potable water distribution systems in general. In the report of Water Quality Research Foundation (WQRF) [6], it is estimated that the heat transfer efficiency of instantaneous gas water heaters reduced by 30% over a 15-year lifecycle if hard water is used.

Both potable and surface water contain a variety of ionic species that contribute to the formation of different types of inorganic deposits in water distribution systems and domestic appliances [7]. Many industries find locations where close access to water sources are available such as rivers, lakes, etc. Heat transfer surfaces come with a tendency to corrode in high temperature conditions [8]. The release of by-product ions such as the cupric ion (Cu^{2+}) in water from copper surfaces may lead to the formation of new types of solid deposits. The formed scales consequently have various morphologies, physical properties and adhesion characteristics. This can make scaling prevention and removal very challenging.

Figure 1 presents a schematic of mineral scaling on heat transfer surface from a reaction between water ionic constituents and/or surface ions. Figure 1 also shows two mechanisms of mineral deposition: transfer of ionic constituents from the bulk solution to the vicinity of the surface, and integration of scale particles on the surface.

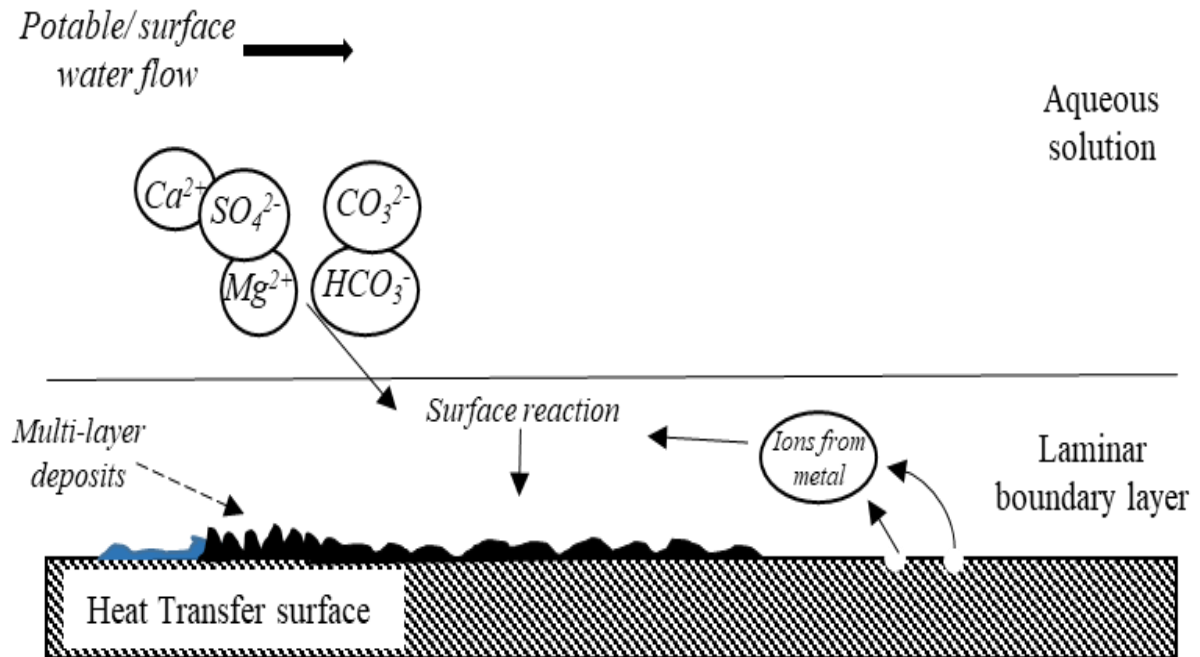


Figure 1. Schematic of surface scaling process from potable water.

Investigations of inorganic scale formation have largely considered the oversaturated solution to study the effect of different parameters on the kinetics and structure of salt deposition. Teng, et al. [9] conducted surface deposition experiments of $CaCO_3$ from artificial fouling solution on five different materials (copper, aluminium, stainless steel, carbon steel and brass) in a counter-current double pipe heat exchanger. Hot water at a constant inlet temperature (50 ± 0.5 °C) is introduced to the inner pipe made of metal, while an artificial fouling solution flows in the outer transparent HDPE pipe of a double pipe heat exchanger. They found that copper has the largest amount of scale deposit and the highest resistance to heat flow, while stainless steel-316 gained the lowest amount of scale and resistance to heat flow under similar conditions. The X-ray diffraction XRD spectrum showed that iron oxide-hydroxide and copper carbonate are also formed on carbon steel and copper, respectively.

The effects of flow velocity on the rate at which a mineral scale can form have been reported [10]. Flow shear stress enhances the removal rate of scale crystals from the heated surface [11, 12], the higher the flow velocity, the lower the resistance to heat transfer [13]. However, the increase of flow velocity promotes the deposition rate of CaCO_3 when flow Reynolds number ranges from 1,457 to 29,135 in a rotating cylinder electrode setup [14]. Wang, et al. [15] performed a study that focused on the effect of flow rate on the scaling behaviour during the induction period in CaCO_3 crystallization fouling on smooth tubes. They demonstrated that the solution flow regime has a positive and negative role in the fouling process. When the flow regime is laminar or transitional, the scaling rate increases rapidly with increasing velocity. On the other hand, under turbulent flow, the increase in flow turbulence reduces the deposition rate and prolongs the induction time [15].

In the present work, the formation of inorganic scale from potable water has been investigated using a once-through in-situ visualization flow rig system during forced convective heat transfer. The surface deposition has been monitored on three different substrates; copper Cu-DHP (C12200), aluminium (1050A) and stainless steel 316L (SS31603). It is anticipated that the scale formed on different materials possesses different compositions and morphologies. Moreover, the influence of solution flow rate has been studied in a laminar flow system. The deposition process has been tested in the presence of vapour bubbles on the heated surface which formed due to the high temperature of the surface.

Experimental methods

Materials

Three metallic cylindrical samples (copper C12200, aluminium 1050A and stainless steel SS31603) with the same surface finish and dimensions of 24 mm (height) and 10 mm (outer diameter) are used. The sample geometry is a one-sided hollow cylinder with an inner diameter of 6.7 mm (Fig.2). The cavity enables the position of a cartridge heater for heating the sample. A 0.5 mm deep channel is made in the internal wall to install the temperature sensor between the heater and sample. The metals selected are the most common materials used in constructing pipes and pools in domestic appliances. The top surface of the sample, which is the tested surface, was grinded with silicon carbide paper (1200 grit) and then polished with diamond suspension (0.5 μm) by a mechanical polishing method. It was subsequently rinsed with acetone, distilled water and dried. The roughness average Ra for the tested surfaces was measured and ranges between 10 to 37.3 nm.

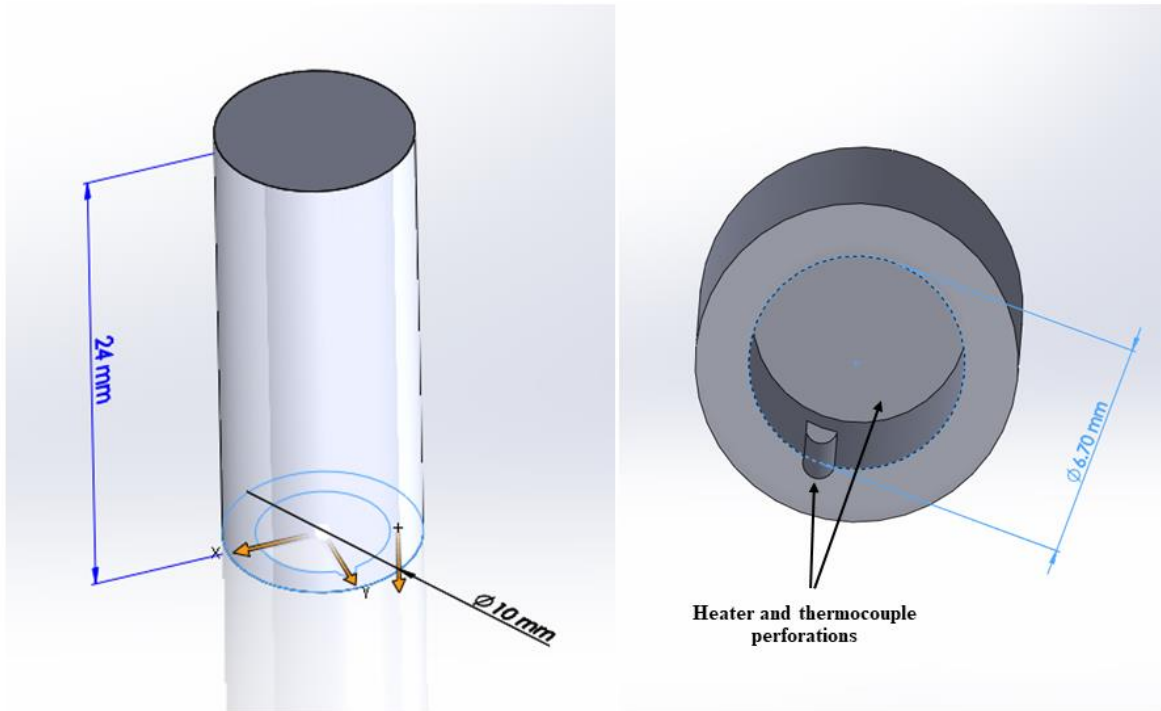


Figure 2. The geometry of a sample used in the experiments

A commercially available bottled water has been used as the fouling test fluid. It has a hardness of 3.07 mmol/L of CaCO_3 and pH of 7.2, which is almost same as potable water hardness in some regions in the south UK. Table 1 shows the specified composition of test water.

Table 1. Composition of the test potable water

Ion	mg/L
Ca ²⁺	80
Mg ²⁺	26
Na ⁺	6.5
K ⁺	1
Si ⁴⁺	15
HCO ³⁻	360
SO ₄ ²⁻	14
Cl ⁻	10
NO ³⁻	3.8
Dry residue at 180 °C	345
SR to aragonite CaCO ₃ at 25 °C	0.92

Apparatus and Procedure

The schematic diagram of the experimental set-up is shown in figure 3. In the present study, the flow is once-through to avoid a decrease in saturation degree with time which may result from fluid circulation [16]. The apparatus mainly consists of a feed tank, pump, flow cell, surface heating system, surface imaging system and waste tank. In the beginning, the test bottled water is transported using a peristaltic digital pump through one line from the feed tank to the flow cell at a controlled flow rate in the laminar flow regime. Across the cell, the flow is uniform with no fluid recirculation [17] and the fluid leaves the cell into the waste tank.

The flow cell (cell volume of 15 ml), where the surface scale forms, is designed to work under atmospheric pressure (Fig. 4). It is built of two polymethylmethacrylate plates (230 mm in length and 70 mm wide) separated by a Teflon sheet with a well-defined channel in the middle. The surface deposition is allowed to be simultaneously monitored through the transparent channel by

a digital imaging machine. Full details of the cell material and dimensions can be found in the work from Sanni [17]. A high-performance monochrome digital camera with 50 frames per second and 1 mega-pixel resolution is connected to a computer to store the surface images at specific time steps for image analysis.

The present work includes a study of the effects of surface material and flow rate on the mineral deposition from potable water. Heat is transferred from the surface to the potable water by the convective heat transfer mechanism. For the investigations of surface material, the flow rate was maintained constant at 4 ml/min (Reynolds number of 7.75). For checking reproducibility, experimental error bars were calculated from the standard deviation of arithmetic mean value for two repeats.

The surface heating is achieved by a stainless-steel cartridge heater (L: 25 mm, OD: 6.5 mm and power: 120W) tightly positioned inside the sample using heat sink compound to eliminate any gap. The cartridge heater temperature is controlled with a proportional–integral–derivative (PID) temperature controller (CAL 9900, UK) with an accuracy of ± 1 °C. The heat flux of the cartridge heater was monitored using a plug-in power monitor (Primera, Brennenstuhl). Two mineral-insulated thermocouple sensors are used; one for the controller feedback signal and the second to make sure the surface temperature is the desired value. The fluid inlet temperature is maintained constant during the experiments at 23 ± 1 °C.

The bulk and cell wall temperatures were measured using digital K-Type thermocouple thermometer (Comark KM330, UK). However, the variation in the bulk and wall temperatures was insignificant.

Surface roughness parameters were evaluated prior to the experiments using the 3D optical profiler NPFlex (Bruker, USA). At the end of every experiment, a sample is removed from the cell, rinsed with distilled water and dried in an oven at 37 °C for 24 hours. A digital laboratory balance (Oxford GM2505D) with an accuracy of ± 1.5 mg is used to determine the mass gain of dried samples. The scale morphology and structure is studied using a Scanning Electron Microscope SEM, Energy Dispersive X-Ray EDX (Carl Zeiss EVO MA15) and Philips X'Pert X-ray diffractometer (Cu anode x-ray source).

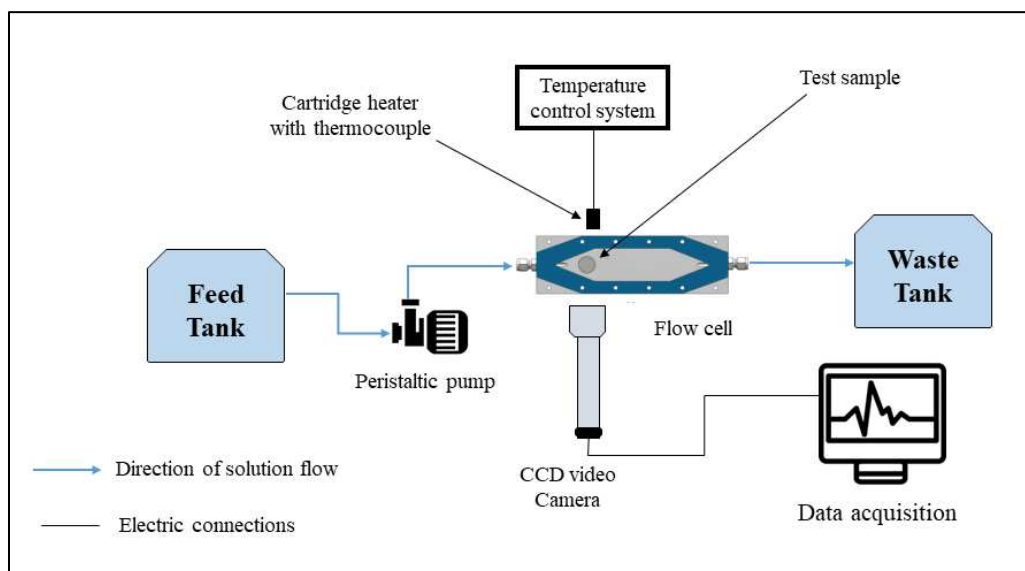


Figure 3. Configuration of the experimental set-up.

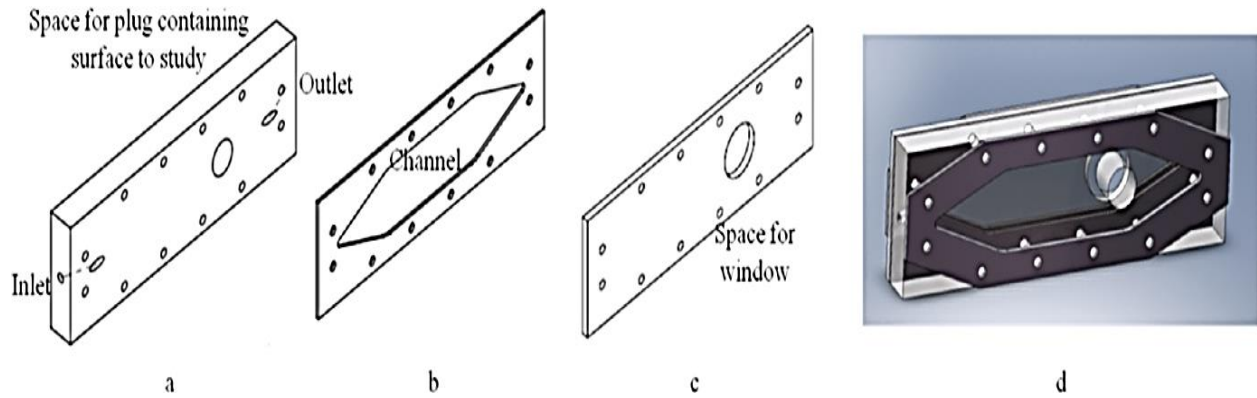


Figure 4. The flow cell is composed of (a) PMMA back plate, (b) Teflon plate, (c) PMMA front plate. (d) The entire body of the cell [18].

Results and Discussion

Effect of surface material

Figure 5 demonstrates the total mineral deposition on S31603, aluminium and copper at a heater temperature of 98.2 °C and initial surface temperature of 90 °C. The thermal conductivity of each metal has been plotted against surface deposition to show how the fouling rate is consistent with the substrate's thermal conductivity. The amount of heat transferred by conduction from the heater and heater temperature are constant during the experiment. Therefore, surface temperature varies based on the material thermal conductivity, the higher the thermal conductivity, the lower the difference between the heater and surface temperatures. Similar findings for the deposition of calcium sulphate on various heat transfer surface materials were obtained by Kazi, et al. [19]. Camera images as shown in figure 6 present the surface coverage after 24 hours of fouling experiment on the tested substrates. Copper is almost covered with scale particles, while few crystals are distributed on the stainless-steel surface.

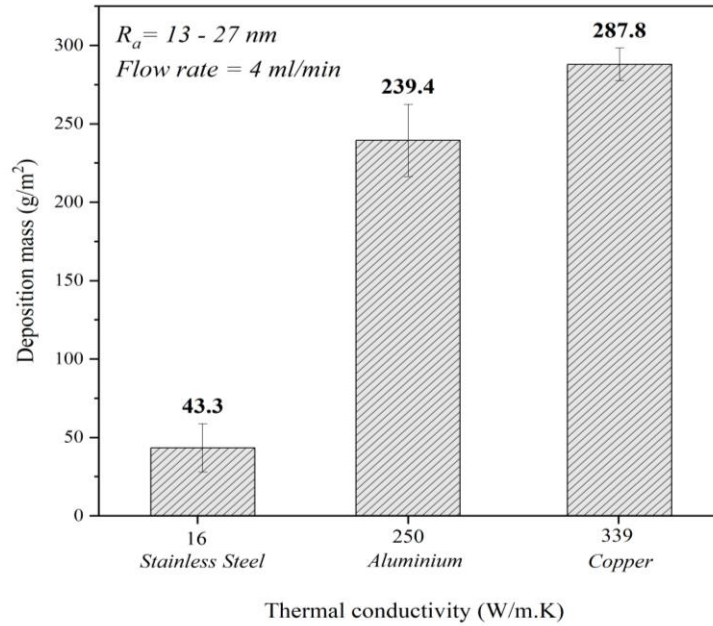


Figure 5. Surface deposition for thermal conductivity of different substrates at a heater temperature of 98.2 °C.

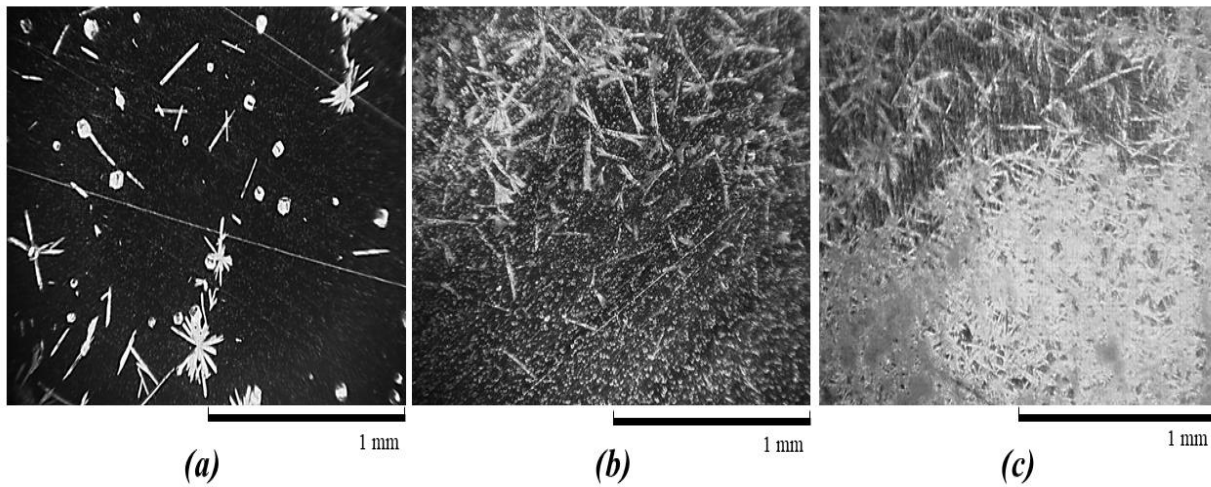


Figure 6. Camera images for scale formation on different substrates: (a) stainless steel; (b) aluminium; and (c) copper, $t = 24 \text{ hrs}$ and $T_h = 98.2 \text{ °C}$.

The results of the EDX analysis of flat smooth deposits on the copper surface are presented in figure 7. The thin layers on the surface are rich with copper and oxygen (Spectra 7 and 8). It can

be concluded that deposited layers are mainly made up of one form of copper oxide which is produced as a corrosion product from the heat transfer surface because the test water contains no Cu ions. Hence, the surface temperature may promote the oxidation reaction. The second scenario is that Cu ions are absorbed into the growth sites of CaCO₃ crystal resulting in growth retardation [20]. The thicker layer mainly comprises calcium, carbon, magnesium and oxygen (Spectrum 6).

The SEM observations in figure 8 show the formation of two different phases of scale; porous rough layer and flat smooth layer of deposits on the tested substrates with the rough part mainly consists of needle-like aragonite. The X-ray diffraction data displayed in figure 9 emphasizes that the crystalline phase of copper oxide (cuprous Cu₂O) is formed on the copper substrate. The findings illustrate that aragonite is the prevailing polymorph of CaCO₃ for the tested substrates and the presence of calcium sulfate as anhydrite is also detected on the copper substrate.

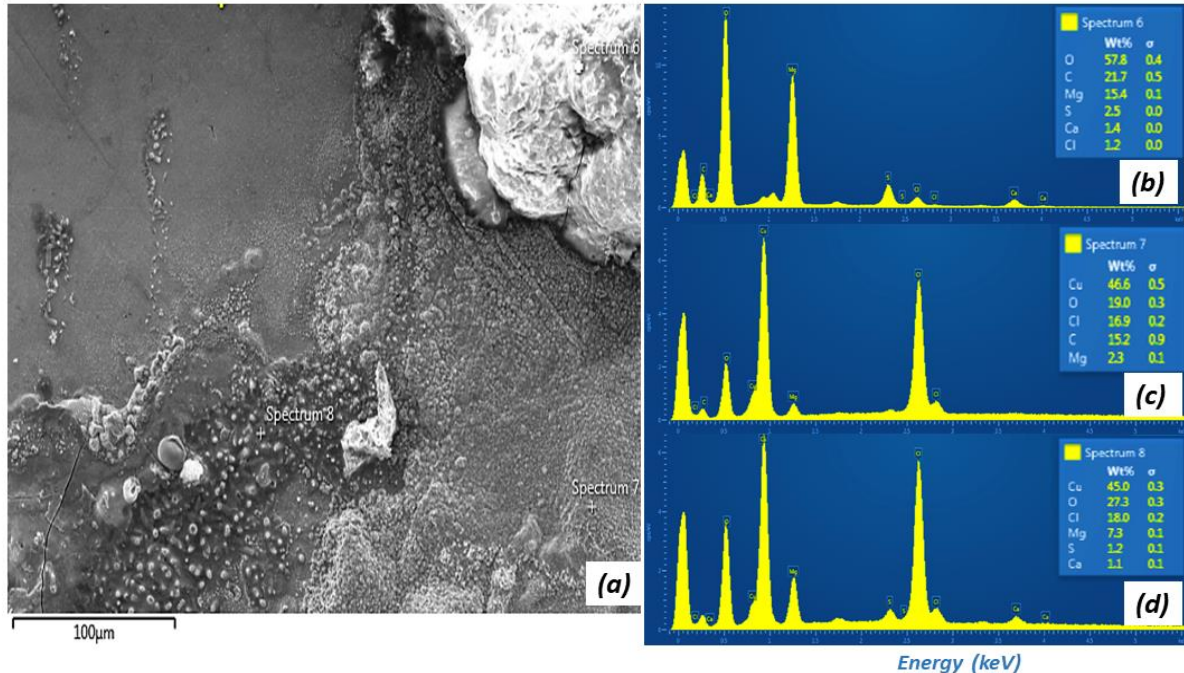


Figure 7. EDX elemental analysis of the mineral scale on copper; (a) SEM image, (b) spectrum 6, (c) spectrum 7 and (d) spectrum 8.

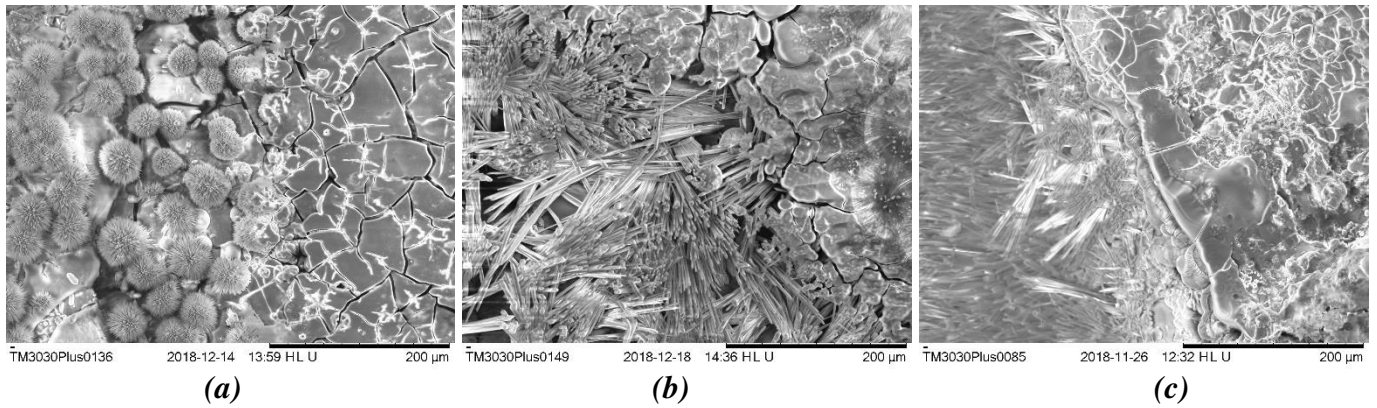


Figure 8. SEM images for scale formation on various heat transfer surfaces: (a) stainless steel; (b) aluminium; and (c) copper.

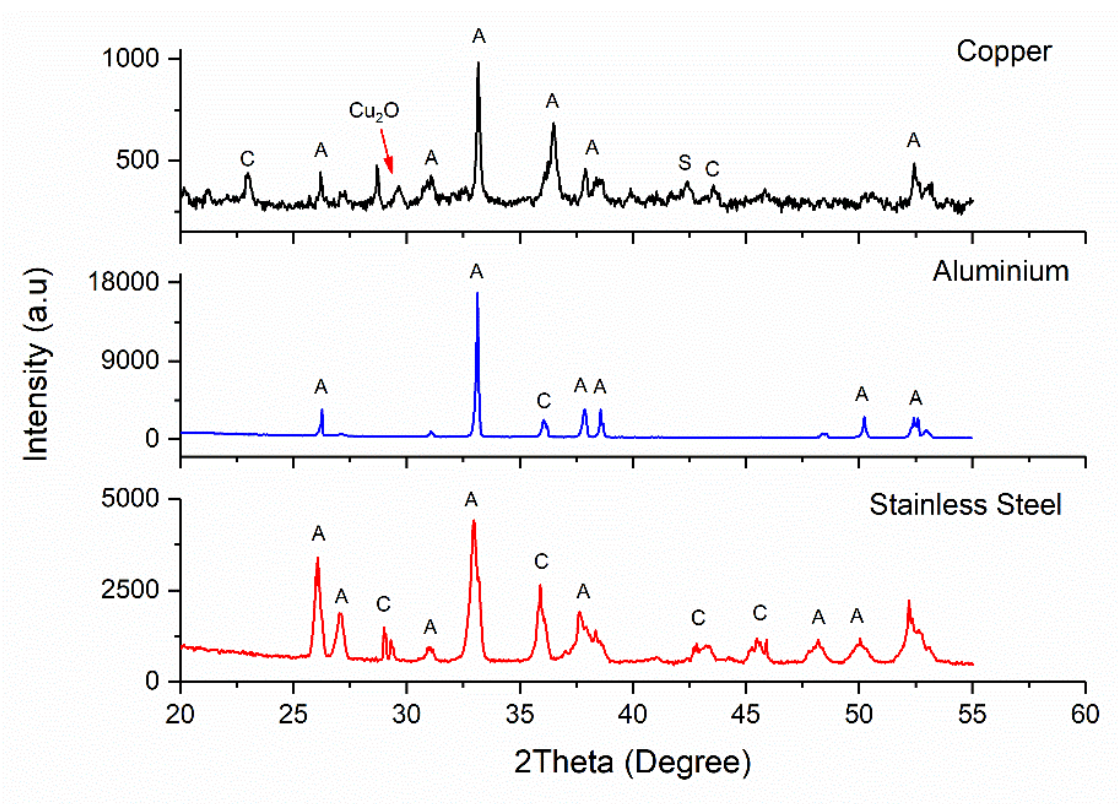


Figure 9. XRD data for the deposited materials on different substrates (A: Aragonite; C: Calcite; and S: Anhydrite calcium sulfate).

Effect of flow rate

The effect of flow rate on surface deposition has been studied using stainless steel substrate at a heater temperature of 98.2 °C, tested flow rates in the range of 0.65 ml/min- 6.32 ml/min corresponding to laminar flow regime with Reynolds numbers 1.26 – 12.07 (Figure 10). Solution flow has a complicated role in crystallization fouling. The increase in flow rate reduces the amount of scale formed on the heat transfer surface until it reaches the optimum point. The optimum point is the flow rate at which the lowest amount of mineral scale is deposited on the heated surface for particular surface characteristics and temperature. At the range below the optimum point, similar to findings obtained by Pääkkönen, et al. [11], flow rate reduces the surface temperature due to enhanced convective heat transfer, hence decreases the crystallization reaction rate and the total deposition. Above the optimum point, the total deposition increases with flow rate. Flow velocity promotes the mass transfer of foulants from the bulk solution to react on the surface. According to the study by Hasson, et al. [21], the mass deposition rate is proportional to the mass transfer coefficient.

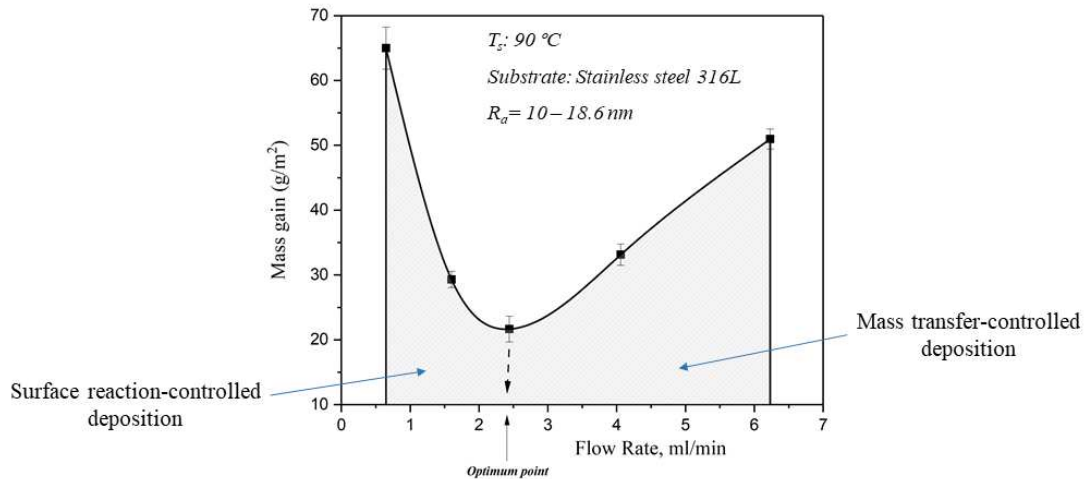


Figure 10. Effect of flow rate on the scale amount on the heat transfer surface.

At lower flow rate, a mixture of needle-like and sunflower-like aragonite calcium carbonate was formed on the stainless steel with the absence of the smooth crystalline layer (Figure 11). The flat smooth fouling layer can be seen in flow rate tests of 4 and 6.32 ml/min. Figure 12 displays the stages of morphological transformation for flower-like aragonite from twin-rosette aragonite, the tiny twin-rosette aragonite particles get taller with time (Figure 12a and 12b). The bristles at ends of the stick-like particle become longer and denser, and start bending to approach those at the other end (Figure 12 c and 12d) until a complete flower-like particle forms and grows to larger flowers (Figure 12e and 12f). The above process allows the surface to be fully covered by a dense layer of flower-like aragonite which has a greater surface area than the twin-rosette.

The XRD data shows a morphological transformation of CaCO_3 crystallite from aragonite to calcite with an increase in flow rate (Figure 13). Magnesium hydroxide, as brucite is detected on the surface under a water flow rate of 6.23 ml/ min.

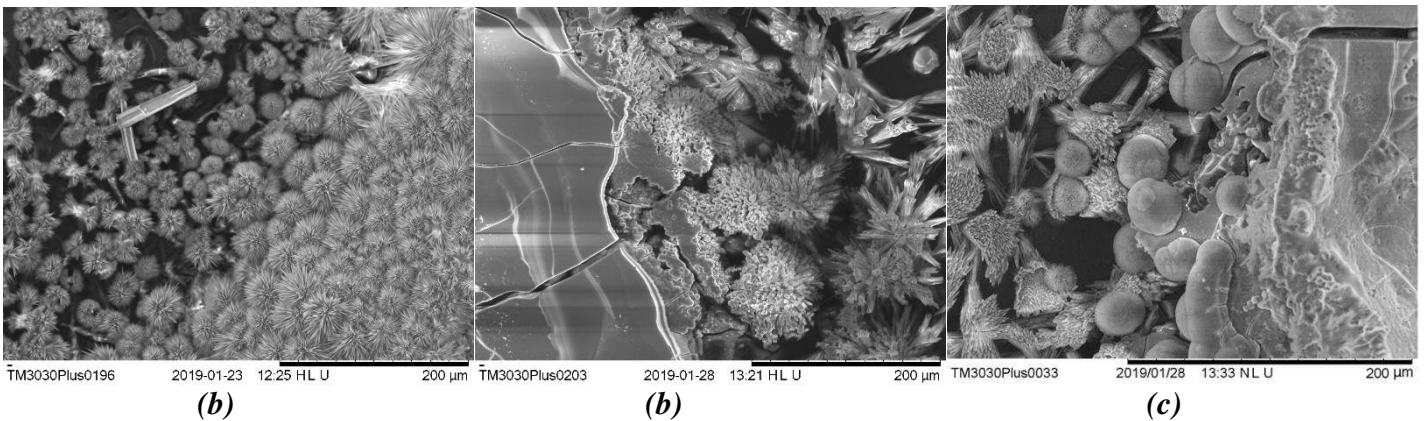


Figure 11. SEM images of scale particles under effect of various flow rate: (a) $0.65 \text{ ml}\cdot\text{min}^{-1}$; (b) $4 \text{ ml}\cdot\text{min}^{-1}$; and (c) $6.23 \text{ ml}\cdot\text{min}^{-1}$.

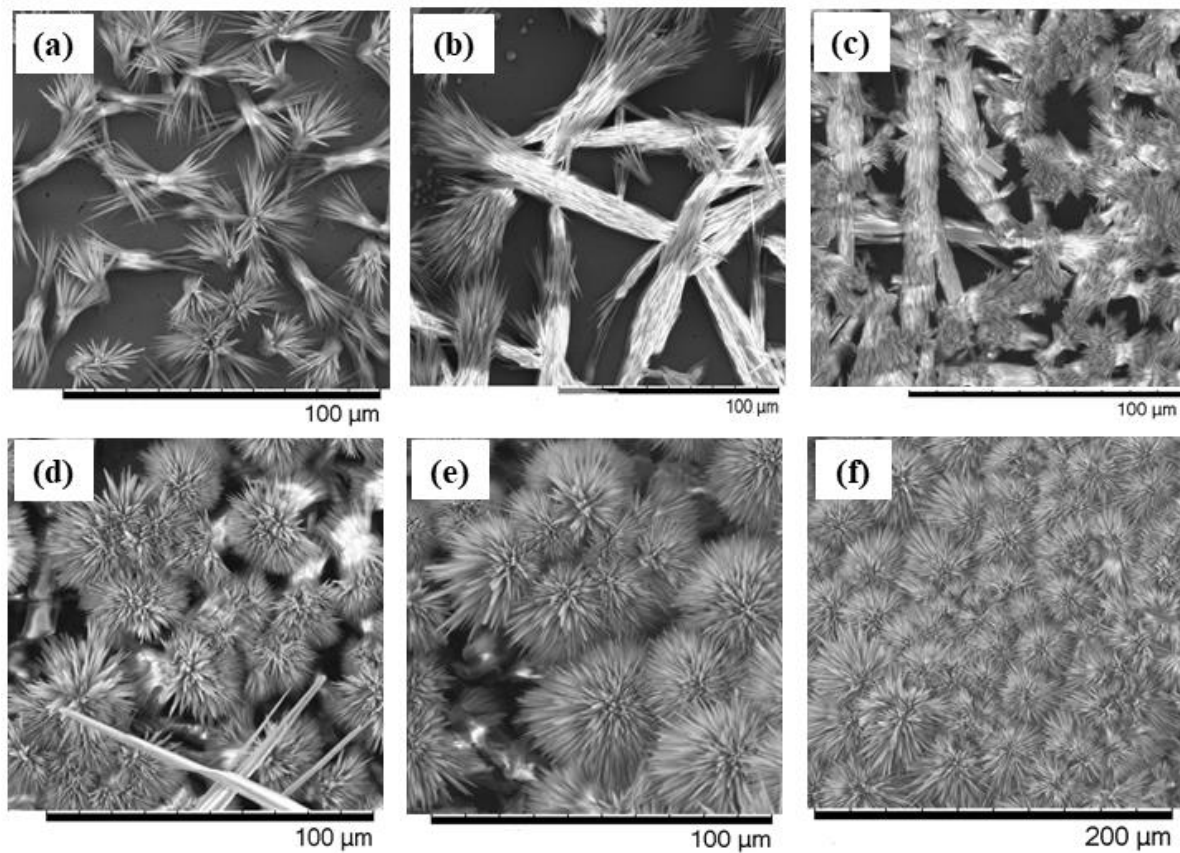


Figure 12. SEM observations of CaCO₃ morphology transformation on stainless steel with time under a flow rate of 0.65 ml.min⁻¹: (a-c) a twin-rosette aragonite at different growth stages; and (d-f) a flower-like aragonite.

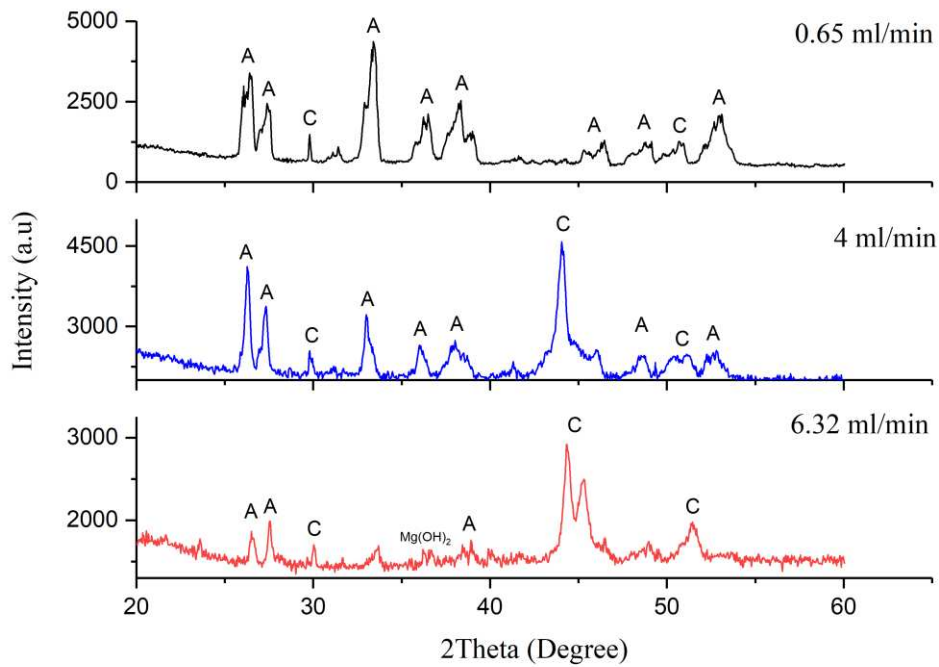


Figure 13. XRD data for the deposited minerals under the effect of different flow rate (A: Aragonite and C: Calcite).

Conclusions

The effect of two parameters was studied in order to provide an appropriate understanding of inorganic fouling from potable water. As potable water contains a variety of ionic species, deposits with different morphologies and compositions were formed on the heat transfer surface. Concerning the substrate effect, copper and stainless steel gained the largest and smallest amount of scale deposits, respectively, while the amount of scale formed on aluminium is closer to the amount on copper than stainless steel. Two distinct scale regions are observed on the surface under different temperatures, the first is the flat Mg-rich layer and the second is a rough scale layer of calcium carbonate. However, copper and oxygen are observed as a thin deposited layer in some

regions of the copper surface. The presence of copper (I) oxide on the copper surface is confirmed by the XRD measurement.

Fluid flow has a complicated role in the fouling rate. Flow rate reduces the amount of scale formed per unit area reaching the optimum point, at which the lowest scale mass is obtained. Above the optimum point, the total deposition increases with the flow rate increase. In terms of scale morphology, aragonite is the dominating polymorphic phase of CaCO_3 under all test conditions.

Acknowledgements

The authors acknowledge the funding and support from the Leeds University SALSAS consortium. We also acknowledge the financial support of the Leverhulme Trust Research Grant ECF-2016-204. We also wish to acknowledge the technical and administrative team of the Institute of Functional Surfaces (IFS), School of Mechanical Engineering at the University of Leeds for their supports.

Nomenclature

<i>A</i>	Aragonite	<i>S</i>	Calcium Sulfate Anhydrite
<i>C</i>	Calcite	<i>SEM</i>	Scanning Electron Microscope
<i>EDX</i>	Energy Dispersive X-Ray	<i>V</i>	Vaterite
<i>Ra</i>	Roughness average	<i>XRD</i>	X-ray Diffraction
<i>T_s</i>	Surface temperature (°C)	<i>t</i>	Time (hr)
<i>T_h</i>	Heater temperature (°C)	<i>SR</i>	Saturation ratio

References

- [1] R. Sheikholeslami, "Composite Fouling of Heat Transfer Equipment in Aqueous Media - A Review," *Heat Transfer Eng.*, vol. 21, no. 3, pp. 34-42, Jul. 2000. doi: <https://doi.org/10.1080/014576300270889>.
- [2] O. Bukuaghangin *et al.*, "Kinetics study of barium sulphate surface scaling and inhibition with a once-through flow system," *J. PETROL. SCI. ENG.*, vol. 147, pp. 699-706, Nov. 2016. doi: <https://doi.org/10.1016/j.petrol.2016.09.035>.
- [3] A. Al-Gailani *et al.*, "Inorganic Mineral Precipitation from Potable Water on Heat Transfer Surfaces," *J. Cryst. Growth*, p. 125621, Mar. 2020. doi: <https://doi.org/10.1016/j.jcrysgro.2020.125621>.
- [4] B. O. Hasan, E. A. Jwair, and R. A. Craig, "The effect of heat transfer enhancement on the crystallization fouling in a double pipe heat exchanger," *Experimental Thermal and Fluid Science*, vol. 86, pp. 272-280, 2017/09/01/ 2017. doi: <https://doi.org/10.1016/j.expthermflusci.2017.04.015>.
- [5] S. K. Saha, H. Ranjan, M. S. Emani, and A. K. Bharti, "Fouling on Various Types of Enhanced Heat Transfer Surfaces," in *Introduction to Enhanced Heat Transfer*: Springer, 2020, pp. 83-95.
- [6] W. Q. R. F. (WQRF), "Softened Water Benefits Study (Energy and Detergent Savings)," *Lisle, IL: Water Quality Association.*, 2011.
- [7] A. Al-Gailani *et al.*, "Examining the effect of ionic constituents on crystallization fouling on heat transfer surfaces," *International Journal of Heat and Mass Transfer*, vol. 160, p. 120180, 2020/10/01/ 2020. doi: <https://doi.org/10.1016/j.ijheatmasstransfer.2020.120180>.
- [8] N. Boulay and M. Edwards, "Role of temperature, chlorine, and organic matter in copper corrosion by-product release in soft water," *Water Res.*, vol. 35, no. 3, pp. 683-690, Feb. 2001. doi: [https://doi.org/10.1016/S0043-1354\(00\)00320-1](https://doi.org/10.1016/S0043-1354(00)00320-1).
- [9] K. Teng *et al.*, "Calcium carbonate fouling on double-pipe heat exchanger with different heat exchanging surfaces," *Powder Technol.*, vol. 315, pp. 216-226, Jun. 2017. doi: <https://doi.org/10.1016/j.powtec.2017.03.057>.
- [10] S. Alsadaie and I. M. Mujtaba, "Crystallization of calcium carbonate and magnesium hydroxide in the heat exchangers of once-through Multistage Flash (MSF-OT) desalination process," *Computers & Chemical Engineering*, vol. 122, pp. 293-305, 2019/03/04/ 2019. doi: <https://doi.org/10.1016/j.compchemeng.2018.08.033>.

- [11] T. Pääkkönen, M. Riihimäki, C. Simonson, E. Muurinen, and R. Keiski, "Crystallization fouling of CaCO₃—Analysis of experimental thermal resistance and its uncertainty," *Int. J. Heat Mass Transfer*, vol. 55, no. 23-24, pp. 6927-6937, Nov. 2012. doi: <https://doi.org/10.1016/j.ijheatmasstransfer.2012.07.006>.
- [12] M. Mayer *et al.*, "The impact of crystallization fouling on a microscale heat exchanger," *Exp. Therm Fluid Sci.*, vol. 40, pp. 126-131, Jul. 2012. doi: <https://doi.org/10.1016/j.expthermflusci.2012.02.007>.
- [13] A. Vosough, S. M. Peyghambarzadeh, and M. R. Assari, "Influence of thermal shock on the mitigation of calcium sulfate crystallization fouling under subcooled flow boiling condition," *Appl. Therm. Eng.*, vol. 164, p. 114434, Jan. 2020. doi: <https://doi.org/10.1016/j.applthermaleng.2019.114434>.
- [14] A. Quddus and L. M. Al-Hadhrami, "Hydrodynamically deposited CaCO₃ and CaSO₄ scales," *Desalination*, vol. 246, no. 1-3, pp. 526-533, Sept. 2009. doi: <https://doi.org/10.1016/j.desal.2008.11.005>.
- [15] L.-C. Wang *et al.*, "Relationships between the characteristics of CaCO₃ fouling and the flow velocity in smooth tube," *Exp. Therm Fluid Sci.*, vol. 74, pp. 143-159, Jun. 2016. doi: <https://doi.org/10.1016/j.expthermflusci.2015.12.001>.
- [16] O. Sanni, T. Charpentier, N. Kapur, and A. Neville, "Study of surface deposition and bulk scaling kinetics in oilfield conditions using an in-situ flow rig," in *NACE-International Corrosion Conference Series*, 2015, vol. 2015, no. 5916: Leeds.
- [17] O. S. Sanni, "Calcium carbonate surface/bulk scaling mechanisms and kinetics in a once-through in-situ flow visualization rig," Ph.D. dissertation, Dept. MECH. ENG., University of Leeds, 2016.
- [18] V. Eroini, "Kinetic study of calcium carbonate formation and inhibition by using an in-situ flow cell," Ph.D. dissertation, Dept. MECH. ENG., University of Leeds, 2011.
- [19] S. N. Kazi, G. G. Duffy, and X. D. Chen, "Mineral scale formation and mitigation on metals and a polymeric heat exchanger surface," *Appl. Therm. Eng.*, vol. 30, no. 14, pp. 2236-2242, Oct. 2010. doi: <https://doi.org/10.1016/j.applthermaleng.2010.06.005>.
- [20] K. Zeppenfeld, "Prevention of CaCO₃ scale formation by trace amounts of copper (II) in comparison to zinc (II)," *Desalination*, vol. 252, no. 1-3, pp. 60-65, Mar. 2010. doi: <https://doi.org/10.1016/j.desal.2009.10.025>.
- [21] D. Hasson, M. Avriel, W. Resnick, T. Rozenman, and S. Windreich, "Mechanism of calcium carbonate scale deposition on heat-transfer surfaces," *Industrial & Engineering Chemistry Fundamentals*, vol. 7, no. 1, pp. 59-65, Feb. 1968. doi: <https://doi.org/10.1021/i160025a011>.